ELSEVIER

Surface Science 447 (2000) 156–164

surface science

www.elsevier.nl/locate/susc

Electronic structure of the C defects of Si(001) measured by scanning tunneling spectroscope at room and low temperature (80 K)

K. Hata, S. Ozawa, Y. Sainoo, K. Miyake, H. Shigekawa *

Institute of Applied Physics and CREST, Japan Science and Technology Corporation (JST), University of Tsukuba, Tennodai 1-1-1, Tsukuba 305-8573, Japan

Received 8 May 1998; accepted for publication 12 November 1999

Abstract

We have studied the electronic characteristics of the C defects of Si(001) by scanning tunneling microscopy (STM) and spectroscopy at 80 K and room temperature. At room temperature, the C defects had a metallic feature as reported before. However, at 80 K, the C defects that do not act as phase shifters were found to have a metallic feature similar to those at room temperature, while the C defects that act as phase shifters have a semiconductive feature with a band gap of −0.5 V. This indicates that the buckled dimers surrounding the C defects influence and change the electronic structure of the C defects at low temperature. When compared with the buckled dimers, the semiconductive C defects have a state with strong intensity located 0.5 V above the Fermi level and the metallic C defects have a prominent state just above the Fermi level. These states are the origin of the appearance of the C defects as bright protrusions in the empty state STM images.

Keywords: Scanning tunneling microscopy; Scanning tunneling spectroscopies; Silicon; Surface defects; Surface electronic phenomena (work function, surface potential, surface states, etc.)

1. Introduction

The first scanning tunneling microscopy (STM) observation of a clean Si(001) surface carried out by Tromp et al. [1] at room temperature, not only gave the first direct evidence of dimerization of the top layer Si atoms, but also showed that there exists a rather large number of atomic-scale defects on the surface. Subsequent, scanning tunneling microscopy (STM) observations of clean Si(001) surface also showed certain amounts of defects. Hamers classified these defects into three types, A, B, and C defects [2].

Among these, the C defects are the most interesting [2–8]. Whereas the A and B defects are surface dimer vacancies called missing dimer defects, the C defects appears as two protrusions along the dimer row direction on one side of the dimer row and a depression on the other side. The appearance of the protrusions is dependent on the surface voltage: they appear brighter than the surrounding dimers in the empty state STM images while as darker in the filled state images taken at usual surface biases (∼ −2 V) [3] as shown in the STM images and schematically in Fig. 1. Defects which

* Corresponding author. Institute of Applied Physics, University of Tsukuba, Tennoudai 1-1-1, Tsukuba 305, Japan. Tel.: +81 298 536469; fax: 81 298 557440; http: //dora.ims.tsukuba.ac.jp.

E-mail address: hidemi@ims.tsukuba.ac.jp (H. Shigekawa)

0039-6028/00/$ - see front matter
PII: S0039-6028(99)01166-8

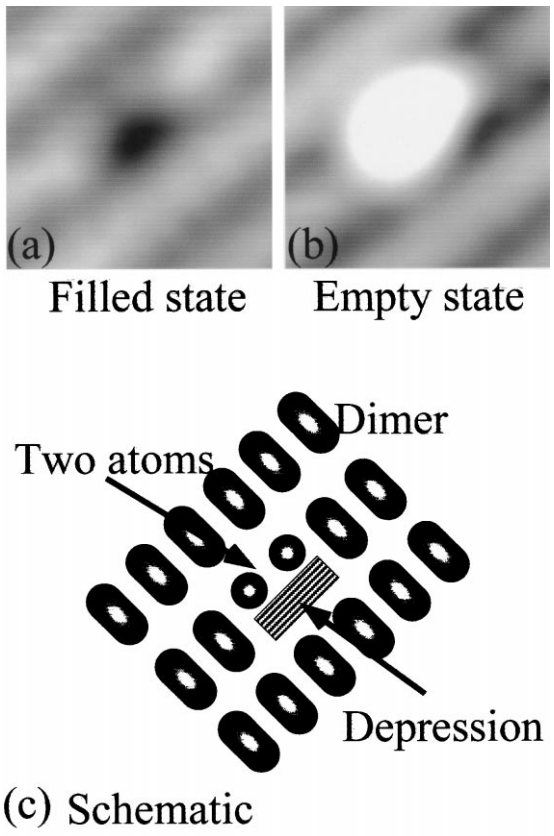

Fig. 1. (a) Filled state STM image ($V=-1.5$ V, $I=1$ nA) of the C defect. (b) Corresponding empty state STM image ($V=+0.6$ V, $I=1$ nA). (c) Stick and ball structure model of the C defect.

show these characteristics in the STM images are defined as the C defects in this study. Other reported characteristics of the C defects are as follows. Tunneling I–V measurements on the C defects show a metallic feature [2,4,5]. Regarding the rather high concentration of C defects, they are considered to be the prominent cause of Fermi level pinning [2]. Also, the C defects are frequently observed to influence the adsorption sites; for example, the C defects are sensitive to oxidation [4,6]. The C defects are reported to show a complicated structural transformation which differs at room temperature [3,7] and low temperature (80 K) [8]. These features make it clear that the C defects play a leading role in characterizing the surface [2].

The configuration of the surrounding dimers is another factor which must be considered. Nowadays, it is generally accepted that STM images at room temperature predominantly show symmetric dimers because STM is imaging the time average of the flip-flop motions of the dimers. Indeed, at low temperatures, the flip-flop motion is frozen and the dimers appear as buckled in the STM images [9–11]. Whether dimers are buckled or not is a factor which has to be considered seriously. In a previous paper, we have shown that A and B defects can be, at least, divided into three sub-categories at low temperatures depending on the fashion of buckling of dimers adjacent to the defects [12]. Turning to the C defects, they seem to have a contradictory influence on the surrounding dimers at room and low temperatures. At room temperature, dimers adjacent to the C defects are observed as buckled [1,2]. Buckled dimers are induced by the C defects at room temperature. In contrast, at low temperature (140 K), dimers at one side of the C defects appear as buckled while those at the other side as symmetric [11]. This is due to an inherent nature of the C defect, i.e., a phase shifter [11]. Schematically the C defect can be considered to be two adjacent dimers buckled in the same direction (ferromagnetic ordering), hence disorganizing the antiferromagnetic ordering of the buckled dimers at low temperature. In this sense, it would be interesting to study and compare the properties of the C defects at room and low temperatures.

In this paper, we present details of the electronic structure of the C defects measured by scanning tunneling spectroscopy (STS) at room and low temperatures (80 K) where dimers are observed as buckled. At room temperature, all of the C defects measured showed a metallic behavior as reported before. In contrast, at low temperature (80 K), we found C defects showing a semiconductive behavior as well as the metallic C defects. The ordering of the surrounding buckled dimers seems to be very important, and characterizes the electronic structure of the C defect. In addition, we measured the spatial distribution of the electronic structures of the semiconductive C defects at low temperature, showing that the electronic structure of the C defects possesses a plane symmetry perpendicular to the dimer row direction.

2. Experimental

Si samples were phosphorus doped with a conductivity of 0.005 Ω cm. After the sample had been prebaked at ~700°C for one night, it was flashed once to 1250°C for 30 s, followed by annealing at 700°C for another 30 s. The base pressure was kept under 5×10^{-8} Pa during flashing. Electrochemically etched tungsten tips were used for the STM and STS measurements.

3. Results

Tunneling spectroscopic measurements at low temperature (80 K) show that the C defects have different electronic characteristics at low and room temperatures.

First we present results obtained at room temperature for comparison. Before measuring the tunneling *I–V* characteristics, identification of the C defects was done by scanning the target defect with both positive and negative bias voltage, and confirming that the target defect shows the characteristics of the C defect. The full line in Fig. 2a shows a typical tunneling *I–V* spectrum of the C defects at room temperature. Tunneling *I–V* spectra of the Si(001) dimers were taken with the same tip and are displayed as the dashed lines. They were taken to confirm that the measurements are not influenced by the electronic structure of the tips as mentioned in details in the following. The Fermi level is at the edge of the conduction band, because the sample is n-type. As reported before, the C defects at room temperature always show a metallic *I–V* characteristic [2,4,5] while the dimers show a semiconductive behavior.

In contrast, at low temperature, the situation becomes different. As mentioned in Section 1, an isolated C defect must act as a phase shifter in a complete set of buckled dimers, an example shown in Fig. 3a. However, STM observations carried out at low temperature show that not all of the C defects act as phase shifters, an example being shown in Fig. 5. (It should be noted that STM images shown in this article are those of the empty states.) In these cases, usually, there exists a peculiar structure adjacent to the C defects which absorbs

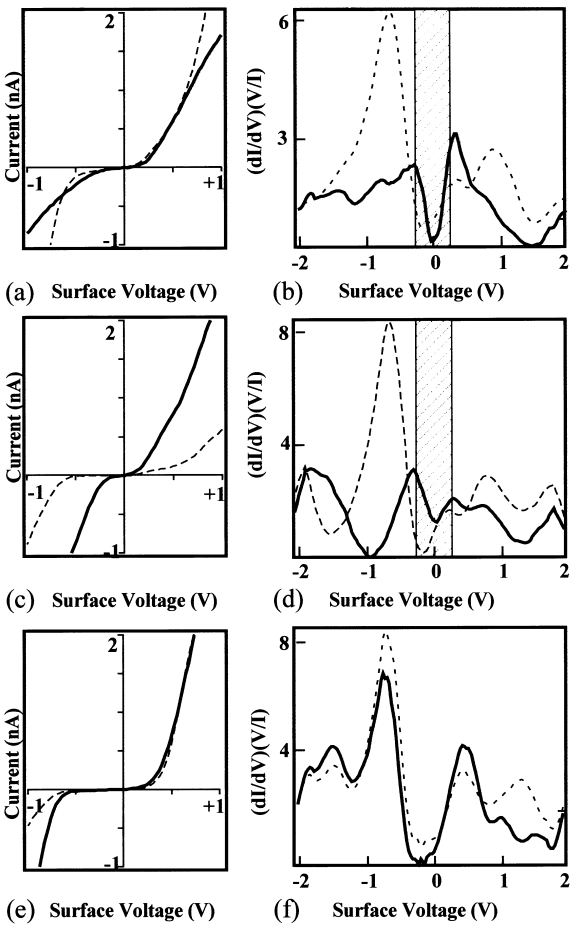

Fig. 2. (a, b) An *I–V* curve and STS spectra of the C defects at room temperature. (c, d) An *I–V* curve and STS spectra of the C defects at 80 K that are not phase shifters. (e, f) An *I–V* curve and STS spectra of the C defects at 80 K that are phase shifters. The dashed lines in each figure show the *I–V* curves and STS spectra of the dimers taken with the same tip apex with which the corresponding C defect was measured.

the effect of the C defect to act as a phase shifter as shown in Fig. 5. We found that the two types of C defects have very different electronic structures. Fig 2c and e shows typical tunneling *I–V* spectra of the C defects that are not and are phase shifters at low temperature, respectively. Tunneling *I–V* spectra of the Si(001) dimers were taken with the same tip and are displayed as the dotted lines. It is easy to see that in each case the dimers show a similar semiconductive behavior with a band gap of ~0.5 V. The C defects that are not phase shifters

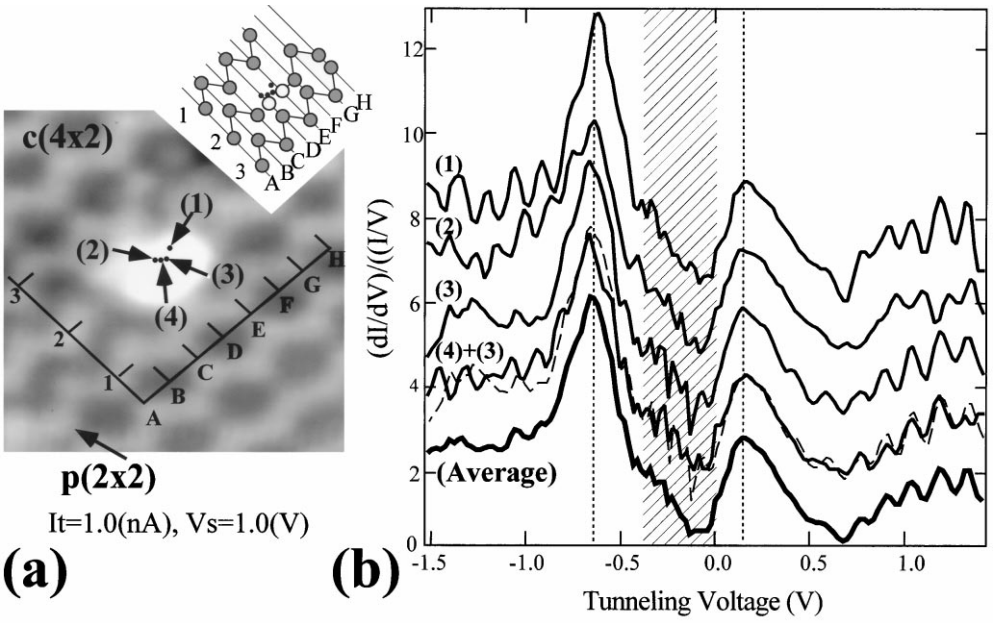

Fig. 3. (a) An STM image of a C defect on which the spectroscopic measurements were performed. Tunneling voltage 1 V, current 1 nA. The inset shows the stick and ball atomic structure of the dimers and the C defect. Note that in the inset the lower atom of the buckled dimer is displayed as a circle because the surface bias of the STM image is positive, and hence the lower atom of the buckled dimer is observed. The black circles in the inset shows the locations where the STS measurements were carried out. (b) A set of tunneling spectra $(dI/dV)/[(I/V)$ versus $V]$ taken at the center of the C defect, curves (1)–(4), and the averaged spectrum, curve (Average), with an offset applied. Spectrum (4), full line, is overlapped with spectrum (3), dashed line.

show a metallic I–V characteristic similar to the C defects at room temperature, while those that act as phase shifters show a semiconductive I–V characteristics similar to the dimers.

The normalized tunneling conductivities (STS spectra, $(dI/dV)/(I/V)$ versus V) are numerically calculated from the I–V curves as displayed in Fig. 2b, d and f. Reliability of the STS measurements was addressed by the following procedure. By analyzing many independent STS runs, we found that a given tip will provide reproducible STS spectra, though a different tip apex might provide quite different spectra. In some extreme cases, even a metallic dimer was observed. It is clear that the STS spectra are influenced by the electronic structure of the tip as reported previously [13,14]. We also found that the STS spectra of the dimer are rather place insensitive, i.e., every dimer gives similar STS spectra. Therefore, we measured the STS spectra of the dimers with the same tip apex each time we carried out the STS measurements on the C defects, and checked that each STS spectrum of the dimers had a similar shape to that which is believed to reflect the true electronic structure of the dimers, i.e., the STS spectrum reported by Hamers et al. [15]. Tips which do not provide this 'right dimer spectra' were abandoned. The dotted lines in Fig. 2b, d and f are the measured STS spectra of the dimers which we have classified as the 'right dimer spectra'. The 'right dimer spectrum' is characterized by one pronounced peak in the filled state between -0.7 and -0.8 V with an intensity of 5–8, a bandgap of ~ 0.5 V, and some peaks in the empty states with an intensity of around 3–4 (not always clearly resolved). The overall shapes of the three 'right dimer spectra' in Fig. 2 show good coincidence, which means that the STS measurements are carried out under the same conditions, i.e., the tips had a similar electronic structure in each case. There exist some discrepancies among the small peaks in the 'right dimer spectra' in

Fig. 2 which sets the upper limit of the reliability of the STS measurements. In particular, the intensity of the peaks of the empty state strongly depends on the tips. Therefore, in the following we will concentrate on and discuss only the overall trend of the spectra.

The normalization procedure of the tunneling current seriously emphasizes the tunneling noise (several pA) around the Fermi level, preventing the observation of the intrinsic electronic structure near the Fermi level. The shaded regions in Fig. 2b and d represent the energy window in which no reliable STS signals could be obtained because of the emphasized tunneling noise. We have to investigate the tunneling I–V curves and the un-normalized spectra (the $\mathrm{d}I/\mathrm{d}V$ versus V curves, not shown) to determine whether or not any states are located in this region.

We conclude that the C defects at room temperature and the C defects that do not act as phase shifters at low temperature have a similar metallic electronic structure. Their electronic structure is characterized by one wide state located above the Fermi level spanning from -1 to 1 V with an intensity above ~ 3 (the exact intensity cannot be measured because it is located above the Fermi level). This result was confirmed both at room and low temperature with different tips and defects. The overall intensity of the STS spectra of the metallic C defects is lower than that of the dimers in the filled states. This agrees with the darkening of the C defects in the STM images taken at high voltages. The metallic C defects have a very different electronic structure from the dimers. In contrast, C defects that act as phase shifters at low temperature show a different semiconductive electronic structure which resembles that of the dimers. When compared with the dimers, the semiconductive C defects have the same bandgap, lower intensity in the filled state, and a higher intensity for the peak located just above the bandgap (around ~ 0.5 V) in the empty state as shown in Fig. 2f. This result was also confirmed several times.

We have succeeded in resolving the spatial electronic structures of the semiconductive C defect by a set of extensive STS measurements. STM images of the target C defect and its surroundings is displayed in Figs. 3a and 4b (Figs. 3a and 4b are STM images of the same C defect). Locations where we have carried out spectroscopic measurements are indicated by an arrow. All of the STS measurements shown in Figs. 3 and 4 were taken with the same tip apex. The surrounding dimers were completely buckled. Therefore, the surface reconstruction is $c(4\times 2)$ on the right side of the C defect and $p(2\times 2)$ on the left; the C defect is a phase shifter. Tunneling I–V spectra (not shown) show that the C defect is semiconductive with a bandgap similar to that of the dimers.

Fig. 3b shows four different tunneling spectra taken on top of the C defect, and the average spectrum (Average). No smoothing is applied to the spectra. Overall coincidence of the five spectra is excellent. The locations, height, and shape of the main peaks are very similar. The good coincidence among spectra highlights the high reproducibility of the STS measurements within a given tip. The electronic characteristics of the semiconductive C defect is summarized. In the filled state region, the edge of the valance band (around -0.5 V) is followed by the main peak (occupied main peak) at -0.6 V. In contrast, in the empty state, the edge of the conduction band (around 0 V) is followed by the main peak (unoccupied main peak) at 0.2 V. The existence of this state is the origin of the appearance of the C defect as a bright protrusion when probing the empty states. In the higher voltage region (above 0.6 V) there exists a set of small peaks which are distributed somewhat regularly (oscillation structure). The origin of these regular small peaks will be discussed later.

Fig. 4b shows a set of tunneling spectra taken at different lateral separations from the C defect, and tunneling spectra, curves (8) and (9), of the dimers adjacent to the C defect which belong to the $p(2\times 2)$ and $c(4\times 2)$ phases, respectively. Also for comparison, we show a tunneling spectrum (Ideal) of a dimer taken at the middle of a wide complete $c(4\times 2)$ domain (ideal surface) with the same tip. As we move from the center of the C defect, the tunneling spectrum quickly changes its shape to that of the ideal surface, and the unoccupied/occupied main peak reduces/increases its height. (spectra 5–7). Two spectra of the dimers adjacent to the C defects in the $c(4\times 2)$ and

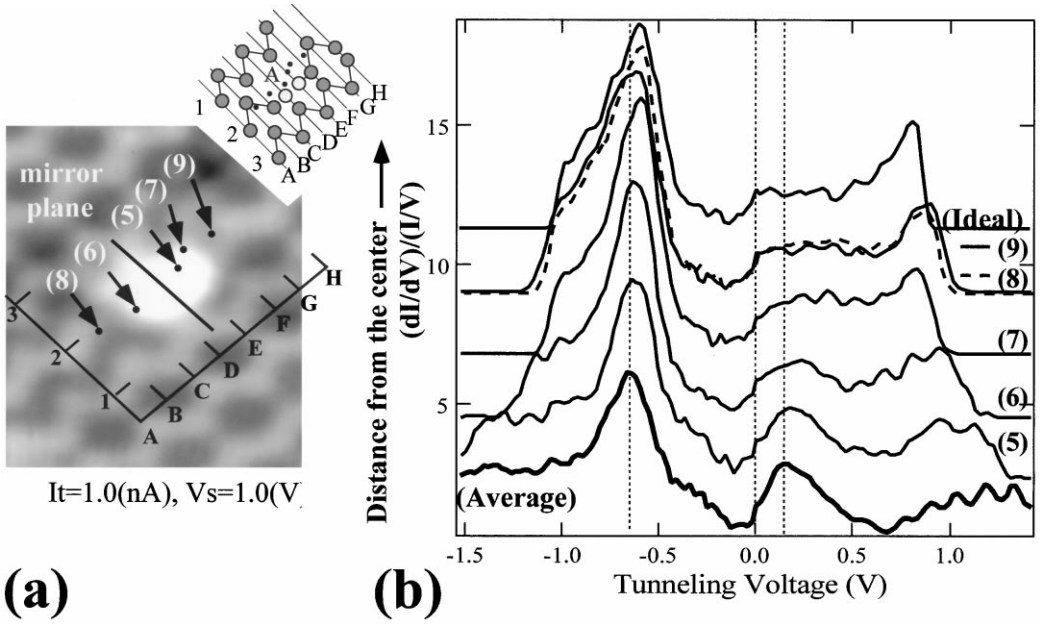

Fig. 4. (a) The same STM image of the C defect shown in Fig. 3. The inset shows the stick and ball atomic structure of the dimers and the C defect. Note that in the inset the lower atom of the buckled dimer is displayed as a circle because the surface bias of the STM image is positive; hence the lower atom of the buckled dimer is observed. The black circles in the inset shows the locations where the STS measurements were carried out and the black circle labeled A represents the mean position where the measurements of Fig. 3 were carried out. (b) Tunneling spectrum of the center of the C defect (Average) with a set of tunneling spectra taken at different lateral separations from the center of the C defect, curves (5)–(9), and tunneling spectra of dimers adjacent to the C defect which belong to the $p(2\times2)$ phase (curve (8), dashed line), and $c(4\times2)$ phases (curve (9), real line), respectively, with an offset applied. For comparison a spectrum taken at the dimer located in the middle of a $c(4\times2)$ domain is shown (Ideal).

$p(2\times2)$ reconstructions (spectra 8 and 9) are similar, although they are different from that of the ideal surface (a smaller peak at 0.7 V). Thus, the C defects influence the electronic structure of the adjacent dimers. Another feature of the C defects is that the electronic structure is highly symmetric regarding the plane parallel to the dimers (the mirror plane is display in Fig. 4a). This is highlighted by the similarity of two spectra, curves (6) and (7), taken on the right and left edges of the C defect. Regarding this high symmetry in the electronic structure, we claim that the real atomic structure of the C defect also possesses this mirror plane.

4. Discussion

In order to understand why some C defects are metallic while others are semiconductive at low temperatures, it is necessary to consider how the C defects influence the ordering of the surrounding buckled dimers. Experiments imply that whether or not the C defects act as phase shifters is the factor that determines the electronic characteristics. Isolated C defects will act as phase shifters when they are placed in a complete set of buckled dimers. These C defects will be highly stressed by the surrounding buckled dimers because they disturb the order of the dimers.

In contrast, we have shown that a certain number of C defects do not act as phase shifters at low temperatures. A typical STM image of the non-phase shifter C defect is displayed in Fig. 5a. It is easy to realize that the C defect is surrounded by a set of buckled dimers with a complete $c(4\times2)$ ordering; thus this C defect does not disturb the ordering of dimers. An inspection of the surface in the vicinity of the C defect reveals the existence of a peculiar atomic structure adjacent to the C

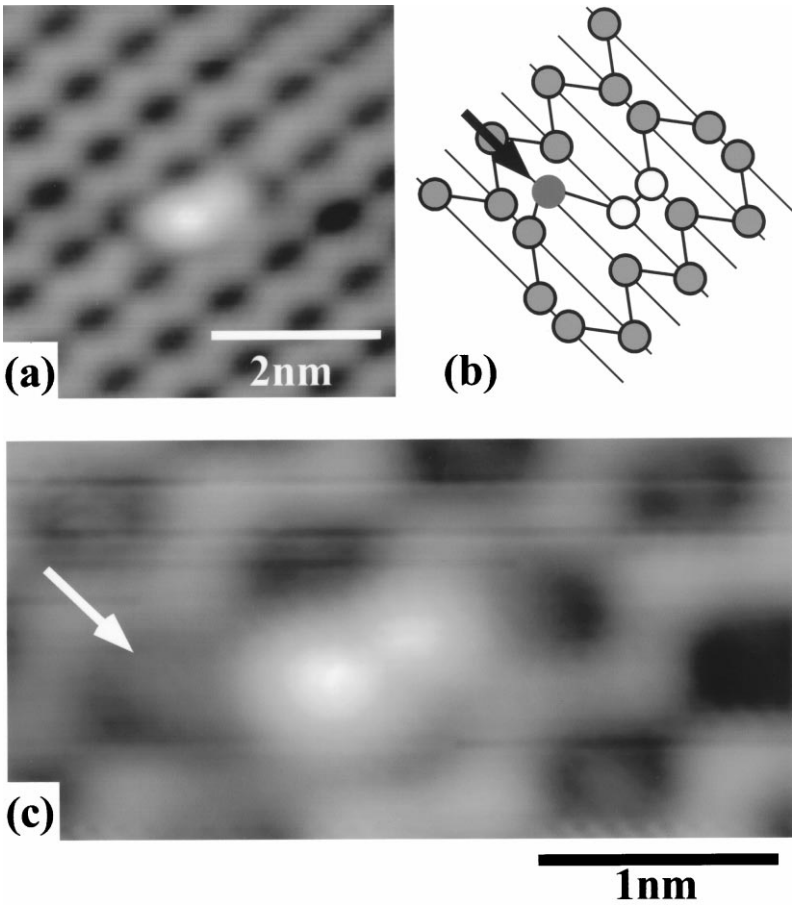

Fig. 5. (a) An STM image ($V=+0.6$ V, $I=1$ nA) of the C defect which does not act as a phase shifter surrounded by a buckled dimer domain with complete c(4×2) ordering. (b) Stick and ball atomic structure of the dimers and the C defect shown in the STM image of (c). The two white atoms represent the C defect, and the gray atom indicated by an arrow indicates the peculiar feature. (c) A high resolution STM image ($V=+0.6$ V, $I=1$ nA) of the C defect and the peculiar structure indicated by an arrow.

defect indicated by the arrow in Fig. 5c. The peculiar atomic feature looks like a dark atom shifted a little towards the next dimer row in the empty states as indicated by the arrow in the image. The stick and ball structure of the C defect with the peculiar feature is displayed in Fig. 5b. At this stage, we do not understand the atomic structure of the peculiar feature. However, as the combination of the C defect and the peculiar feature does not act as a phase shifter, the peculiar feature must represent a defect which acts as a phase shifter (it should be noted that a combination of two phase shifters do not act as a phase shifter). We assume that the combination of the C defect and the peculiar feature is a close combination of a C defect and a P defect. P defects are defects in the ordering of the buckled dimers (two dimers aligned in a ferromagnetic order), and have been directly observed at 6 K [16]. The P defect is a kind of a domain boundary along a dimer row. A close combination of the C defect with a P defect can be understood as a reaction of the surface to reduce the total area of the p(2×2) area which is energetically unfavorable compared with the c(4×2) phase at this temperature [17–19]. Since the P defect is also a phase shifter, a combination of a C defect and a P defect will not act as a phase shifter because each effect as a

phase shifter cancels the other out. What is more important, the combination of the C and P defects will not be stressed by the surrounding buckled dimers because they do not disturb the ordering of the buckled dimers.

In contrast, at room temperature, the buckled dimers are flip-flopping and not static. If the flip-flop motion is such that the correlation length of the buckled dimers is short-ranged, then the C defect will not be stressed from the surrounding dimers. Indeed, at room temperature the dimers adjacent to the C defects are frequently observed as buckled: the C defects stress the adjacent dimers at room temperature. We assume that the C defect is not stressed by the dimers at room temperature and appears as metallic, which we assume to be the natural characteristics of the C defect.

The experimental results might be explained by assuming that the elastic stress field induced by the surrounding buckled dimers influences and changes the electronic structure of the C defects at low temperatures. We assume that, when the C defects do not disturb the ordering of the surrounding buckled dimers, the C defects are not stressed by them, thus remaining as metallic close to their natural characteristics. In contrast, when the C defects act as phase shifters at low temperature, we assume that the stress imposed by the surrounding dimers causes the state at the Fermi level of the metallic C defects to split and result in semiconductive C defects. This means that not only do the defects influence the ordering of the buckled dimers [11,12], but also the electronic (possibly the atomic) structure of the defects is influenced by the ordering of the surrounding buckled dimers.

The C defect is not stable when compared with the dimers [20,21]. Frequently STS measurements would result in a destruction of the C defect. Most of these STS spectra resemble an accumulation of the spectra of the C defect and the dimer with different weighting, overlapped with a regular oscillation similar to that observed in Figs. 3 and 4. We never observed such a perfect set of equally spaced peaks in the STS spectra (Fig. 3b) of the dimers. Therefore, we maintain that the regular oscillations are not due to artifacts such as mechanical oscillation of the tip, but instead that they are due to an oscillation of the uppermost atoms of the C defect induced by the STS measurements. In the extreme cases, this perturbation results in destruction of the C defect.

Finally, we will discuss implications of the results obtained here for the structure models proposed so far. Uda et al. [22] have proposed a structural model of the C defect based on an assumption that the C defects originate from a removal of one atom in the second layer. The calculated local density of states (LDOS) of their structure model (Fig. 3 in Ref. [22]) predicts a semiconductive C defect. However, in their calculation the two types of the C defects (phase shifter or not) were not discriminated and further studies are required to check whether the observed semiconductive–metallic transition occurs when the ordering of the surrounding buckled dimers is considered.

5. Conclusion

In conclusion, we have carried out a detailed STS study to elucidate the characteristics of C defects at low temperatures where most of the flip-flop motions of the dimers were frozen out. In addition to the well-known fact that the C defects influence the ordering of the buckled dimers, we found that the electronic structure of the C defects is also strongly influenced by the surrounding buckled dimers. When the C defects are not stressed they show a metallic behavior which we interpret as reflecting the natural characteristics of the C defects. In contrast, when the C defects disturb the ordering of the surrounding buckled dimers they show semiconductive behavior.

Acknowledgements

This work was supported by the Shigekawa Project of TARA, University of Tsukuba. The support of a Grant-in-Aid for Scientific Research from the Ministry of Education, Science and Culture of Japan is also acknowledged.

References

[1] R.M. Tromp, R.J. Hamers, J.E. Demuth, Phys. Rev. Lett. 55 (1985) 1303.
[2] R.J. Hamers, U.K. Kohler, J. Vac. Sci. Technol. A 7 (1989) 2854.
[3] Z. Zhang, M.A. Kulakov, B. Bullemer, Surf. Sci. 369 (1996) L131.
[4] Ph. Avouris, D. Cahill, Ultramicroscopy 42–44 (1992) 838.
[5] V.A. Ukraintsev, Z. Dohnalek, J.T. Yater, Surf. Sci. 388 (1997) 132.
[6] M. Udagawa, Y. Umetani, H. Tanaka, M. Itoh, T. Uchiyama, Y. Watanaba, T. Yokotsuka, I. Sumita, Ultramicroscopy 42–44 (1992) 946.
[7] K. Hata, S. Ozawa, H. Shigekawa, Surf. Sci. 441 (1999) 140.
[8] K. Hata, R. Morita, M. Yamashita, H. Shigekawa, Jpn. J. Appl. Phys. 38 (1999) 3837.
[9] Y. Nakamura, H. Kawai, M. Nakayama, Phys. Rev. B 55 (1997) 10549.
[10] R.A. Wolkow, Phys. Rev. Lett. 68 (1992) 2636.
[11] H. Tochihara, T. Amakusa, M. Iwatsuki, Phys. Rev. B 50 (1994) 12262.
[12] M. Uchikawa, M. Ishida, K. Miyake, K. Hata, R. Yoshizaki, H. Shigekawa, Appl. Surf. Sci. 357–358 (1996) 468.
[13] R.M. Tromp, E.J. van Loenen, J.E. Demuth, N.D. Lang, Phys. Rev. B 37 (1988) 9042.
[14] T. Klitsner, R.S. Becker, J.S. Vickers, Phys. Rev. B 41 (1990) 3837.
[15] R.J. Hamers, Ph. Avouris, F. Bozso, Phys. Rev. Lett. 59 (1987) 2071.
[16] H. Shigekawa, K. Miyake, M. Ishida, K. Hata, H. Oigawa, Y. Nannichi, R. Yoshizaki, A. Kawazu, T. Abe, T. Ozawa, T. Nagamura, Jpn. J. Appl. Phys. 35 (1996) L1081.
[17] H. Shigekawa, K. Hata, K. Miyake, M. Ishida, S. Ozawa, Phys. Rev. B 55 (1997) 15448.
[18] H. Shigekawa, K. Miyaka, M. Ishida, K. Hata, Jpn. J. Appl. Phys. 36 (1997) L294.
[19] H. Kageshima, M. Tsukada, Phys. Rev. B 46 (1992) 6928.
[20] A. Kobayashi, F. Grey, E. Snyder, M. Aono, Phys. Rev. B 49 (1994) 8067.
[21] K. Hata, M. Ishida, K. Miyake, H. Shigekawa, Appl. Phys. Lett. 73 (1998) 40.
[22] T. Uda, K. Terakura, Phys. Rev. B 53 (1996) 6999.